# Imaging of Bioluminescent LNCaP-luc-M6 Tumors: A New Animal Model for the Study of Metastatic Human Prostate Cancer

Caroline D. Scatena, Mischa A. Hepner, Yoko A. Oei,
Joan M. Dusich, Shang-Fan Yu, Tony Purchio,
Pamela R. Contag, and Darlene E. Jenkins*

*Xenogen Corporation, Alameda, California*

**BACKGROUND.** Animal experiments examining hormone-sensitive metastatic prostate cancer using the human LNCaP cell line have been limited to endpoint analyses. To permit longitudinal studies, we generated a luciferase-expressing cell line and used bioluminescent imaging (BLI) to non-invasively monitor the in vivo growth of primary LNCaP tumors and metastasis.
**METHODS.** LNCaP.FGC cells were transfected to constitutively express firefly luciferase. LNCaP-luc-M6 cells were tested for bioluminescent signal intensity and hormone responsiveness in vitro. The cells were implanted in subcutaneous and orthotopic sites in SCID-bg mice and imaged over time.
**RESULTS.** The LNCaP-luc-M6 cells formed subcutaneous and orthotopic tumors in SCID-bg mice, and nearly all tumor-bearing animals developed pulmonary metastases. Early detection and temporal growth of primary tumors and metastatic lesions was successfully monitored by BLI.
**CONCLUSIONS.** The LNCaP-luc-M6 cell line is a bioluminescent, hormone-sensitive prostate cancer cell line applicable for BLI studies to non-invasively monitor subcutaneous and orthotopic prostate tumor growth and metastasis in vivo. *Prostate 59: 292–303, 2004.*
© 2004 Wiley-Liss, Inc.

KEY WORDS: orthotopic prostate model; biophotonic imaging (BLI); firefly luciferase; mouse xenograft model; micrometastasis

## INTRODUCTION

Prostate cancer is the second leading cause of cancer-related death for men in the United States with more than 220,000 new cases expected this year [1]. While early detection has increased with the advent of serum PSA testing, the disease is often locally advanced or metastatic when patients present with symptoms [2]. Current treatment regimens for metastatic prostate cancer include hormonal therapy, chemotherapy, or radiation either alone or in combination, and these treatments are often only palliative [2,3]. New animal models of prostate cancer that mimic the progression of human disease would be helpful in understanding the molecular mechanisms of disease progression, as well as aid in the development of new therapies.

Several human prostate carcinoma cell lines have been used in animal models, each representing prostate cancer at different disease stages [3–5]. The LNCaP cell line is derived from a human lymph node metastasis and is one of the few hormone-sensitive prostate cancer cell lines currently available [5,6]. LNCaP cells express androgen receptor, secrete PSA, and require steroids for in vitro proliferation [6–9]. The cells grow

as subcutaneous and orthotopic prostate tumors in nude and SCID mice [6,7,10–17], and serum PSA levels have been measured to indirectly monitor tumor growth in vivo [10,12–14,17,18]. When LNCaP cells or tumor fragments are implanted in the prostate of mice, metastases have been identified in the lymph nodes and lungs of the animals post mortem [7,12–14,16]. We have developed a LNCaP cell line expressing luciferase that allows temporal, non-invasive imaging of primary tumor growth and metastasis in vivo in real time.

Over the past decade, advances in small animal imaging have improved the capability to follow disease progression in preclinical models of human cancer [19]. One such advance employs bioluminescent imaging (BLI) to non-invasively monitor the growth of luciferase-expressing carcinoma cells in vivo [20–29]. BLI studies specifically focused on bioluminescent prostate carcinoma cell lines have monitored primarily the growth of androgen-independent tumors and developing metastatic lesions in vivo [25–27]. Only a few BLI studies to date have included androgen-dependent prostate cancer models. For example, LNCaP cells that transiently expressed firefly luciferase have been monitored by BLI in the peritoneal cavity of nude mice [29], and the effectiveness of paclitaxel treatment has been tested in vivo on luciferase-expressing LNCaP intramuscular tumors [27]. Recently, Adams et al. used BLI to monitor the localization of a luciferase-expressing adenovirus to androgen-dependent LAPC4 human prostate tumor xenografts [30].

Our current work complements and expands these previous reports by characterizing a hormone-sensitive LNCaP cell line that constitutively expresses luciferase and can be used to study metastatic prostate cancer in vivo by BLI. We generated a luciferase-expressing LNCaP cell line, LNCaP-luc-M6. We compared the hormone-sensitive phenotype of the LNCaP-luc-M6 cell line to the parental cell line LNCaP.FGC, and we monitored the in vivo growth of LNCaP-luc-M6 tumors at subcutaneous and orthotopic sites in SCID-bg mice. We show that, rather than waiting weeks or months to measure tumor growth by traditional methods, we can monitor tumor growth by BLI beginning 1 week after injection. We detected pulmonary lesions in mice with orthotopic LNCaP-luc-M6 tumors and in mice with subcutaneous LNCaP-luc-M6 tumors, a finding that has previously not been reported. In addition, unlike previous LNCaP studies where metastases were identified post mortem, we show that we are able to monitor the development and growth of metastatic lesions in animals for several weeks in vivo. The data demonstrate the utility of this luciferase-expressing LNCaP-luc-M6 cell line for in vivo imaging applications and as a convenient animal model of longitudinal studies of hormone-sensitive prostate cancer and metastatic disease.

## MATERIALS AND METHODS

### Tumor Cell Lines

The LNCaP.FGC prostate carcinoma cell line was obtained from the American Type Culture Collection (American Type Culture Collection, Rockville, MD). The cell line was cultured in MEM/EBSS (Hyclone, Logan, UT) with 10% fetal bovine serum (Hyclone) and supplemented with L-glutamine, sodium pyruvate, non-essential amino acids (Hyclone), and MEM vitamin solution (Invitrogen, Carlsbad, CA). The cell line was maintained at $37 \pm 2°C$ in a humidified atmosphere containing 5% $CO_2$.

### Plasmid Construction and Transfection

The firefly luciferase (luc) gene was subcloned as a Xho1/Xba1 cDNA fragment from PGL3 (Promega, Madison, WI) into the PCI-Neo expression vector (Promega) putting luciferase expression under the control of the CMV IE enhancer/promoter. Transfection of the LNCaP.FGC cell line was performed using Lipofectamine (Invitrogen), and cells were selected with 300 µg/ml Geneticin (Invitrogen). The surviving colonies were screened for bioluminescence by BLI in vitro using the IVIS® Imaging System as described below (Xenogen Corporation, Alameda, CA). Initially, 48 bioluminescent and antibiotic resistant clones were isolated for expansion into possible stable cell lines. Of those 48, one colony maintained stable expression of luciferase during amplification. The clone, LNCaP-luc-M6 was characterized for stable luminescence expression in vitro and tumorigenic potential in vivo.

### BLI

In vitro and in vivo BLI was performed with an IVIS® Imaging System (Xenogen) comprised of a highly sensitive, cooled CCD camera mounted in a light-tight camera box. Images and measurements of bioluminescent signals were acquired and analyzed using Living Image® software (Xenogen). For in vitro imaging, bioluminescent cells were diluted from 100,000 to 196 cells into appropriate cell culture media in black, clear bottom 96-well plates (Costar, Corning, NY). D-luciferin (Biosynth, International, Inc., Naperville, IL) at 150 µg/ml in media was added to each well, and cells were incubated at 37°C in a humidified atmosphere containing 5% $CO_2$ for 7–10 min prior to imaging for 1 min. For in vivo imaging, animals received D-luciferin at 150 mg/kg in DPBS by intraperitoneal injection at 15 min prior to imaging. The animals were anesthetized using 1–3% isoflurane (Abbott Laboratories,

North Chicago, IL), and placed onto the warmed stage inside the camera box. The animals received continuous exposure to 1–2% isoflurane to sustain sedation during imaging. Imaging times ranged from 10 sec to 3 min, depending on the bioluminescence of the tumors or metastatic lesions. The light emitted from the bioluminescent cells or tumors was detected in vivo by the IVIS® Imaging System, digitized and electronically displayed as a pseudocolor overlay onto a gray scale animal image. Regions of interest (ROI) from displayed images were drawn around the tumor sites and quantified as photons/second (ph/sec) using the Living Image® software (Xenogen). Background bioluminescence in vivo was in the range $3-6 \times 10^4$ ph/sec. For ex vivo imaging, 150 mg/kg D-luciferin was injected into the mice immediately prior to necropsy. Animals were humanely euthanized, tissues of interest excised, and placed individually into 24-well tissue culture plates with 300 μg/ml D-luciferin in DPBS, and imaged for 1 min. Tissues were subsequently fixed in 10% formalin (Sigma, St. Louis, MO) and prepared for standard histopathology evaluation.

### Western Analysis

Cells were lysed in 50 mM Tris, pH 8, 150 mM NaCl, 0.1% SDS, 0.5% Deoxycholate, 1% IGEPAL CA-630 (Sigma), and protease inhibitors from a Complete Protease Inhibitor Cocktail Tablet (Roche, Indianapolis, IN). Protein concentration was determined by the Bradford Assay (Bio-Rad, Hercules, CA), and 25 μg of lysate was separated by SDS–PAGE on 12% Tris-HCl Ready Gels (Bio-Rad). Protein was transferred to Immun-Blot™ PVDF membrane (Bio-Rad). The membrane was incubated with an antibody against the androgen receptor (clone 441, Santa Cruz Biotechnology, Inc., Santa Cruz, CA), followed by incubation in goat anti-mouse horseradish peroxidase conjugated secondary antibody (Pierce, Rockford, IL). Androgen receptor epitopes were detected by chemiluminescence using ECL Plus™ Western Blotting Detection Reagents (Amersham Biosciences, Piscataway, NJ). Equal loading of protein lysates was confirmed with fast green staining of the membrane.

### Proliferation Assays

In duplicate experiments, 20,000 cells/well were seeded on day 0 in a 24-well plate in phenol red-free MEM (Invitrogen) with either 10% fetal bovine serum or 10% charcoal/dextran-treated fetal bovine serum (Hyclone). Both media were supplemented with L-glutamine, sodium pyruvate, non-essential amino acids (Hyclone), and MEM vitamin solution (Invitrogen). The cells were maintained at $37 \pm 2°C$ in a humidified atmosphere containing 5% $CO_2$, and media was

replenished on day 4 and 7. On day 3, 4, 5, 6, 7, and 10, triplicate wells were harvested and the number of cells per well determined using a hemacytometer.

After 4 days of growth in MEM with 10% charcoal/dextran-treated fetal bovine serum, 50% of the wells were fed the same media supplemented with the androgen agonist methlytrienolone (R1881, PerkinElmer, Wellesley, MA) at a concentration of 0.1 nM. Media was refreshed every 3 days. Triplicate wells were harvested 1, 2, 3, and 6 days after the addition of R1881, and the number of cells per well determined using a hemacytometer.

### Mouse Strain and Animal Care

Strict animal care procedures set forth by the Institutional Animal Care and Use Committee based on guidelines from the NIH guide for the Care and Use of Laboratory Animals were followed for all experiments. Animals used in these studies were male, SCID-beige mice (Charles River Laboratories, Wilmington, MA).

### Subcutaneous Tumor Model

Male mice (8–10 weeks old) were administered 150 mg/kg D-luciferin by intraperitoneal injection and were anesthetized with 1–3% isoflurane. Anesthetized animals received $3 \times 10^6$ LNCaP-luc-M6 cells in a subcutaneous injection below the dorsal flank. Cells were suspended in 50% Matrigel™ (Becton Dickinson Labware, Bedford, MA) and sterile DPBS (100 μl final volume). Approximately 15 min after luciferin injection, anesthetized mice were imaged from the dorsal view. Primary tumor growth was monitored weekly for at least 7 weeks by in vivo BLI. Tumor volume caliper measurements ($L \times W \times D$) began 6 weeks after injection. Beginning at week 7, the animals were imaged from dorsal and ventral views. In some images, the lower quadrant of each animal was shielded to minimize the primary tumor bioluminescence so that the relatively lower signals from metastatic lesions could be observed. For ventral images, the forelimbs were also taped down to stabilize the position of mice. The imaging times were 1 min for subcutaneous tumors and 3 min for detection of lung and lymph node metastases.

### Orthotopic Prostate Model

Male mice (8–10 weeks old) were anesthetized by intramuscular injection of 120 mg/kg ketamine hydrochloride (Fort Dodge Animal Health, Fort Dodge, IA) plus 6 mg/kg xylazine (Phoenix Scientific, Inc., St. Joseph, MO), and $1 \times 10^6$ LNCaP-luc-M6 cells suspended in 20 μl sterile DPBS were injected into the dorsolateral prostate lobes after surgical exposure of the prostate. The surgical incision was allowed to heal

1 week before imaging experiments were initiated. For in vivo imaging, the mice received 150 mg/kg D-luciferin by intraperitoneal injection and were anesthetized with 1–3% isoflurane. Fifteen minutes after luciferin injection, mice were placed in the IVIS® Imaging System and imaged from the ventral view. Tumor growth in the prostate was monitored by BLI at weekly intervals for 16 weeks, and imaging times ranged from 10 sec to 1 min depending upon the tumor bioluminescence. Beginning at week 7, the primary tumor was shielded and the animals were imaged for 3 min to monitor metastatic lesion development as described for the subcutaneous model. At the conclusion of the experiment, the animals were humanely euthanized and the prostate tumor was excised and weighed.

### Serum PSA Analysis

Serum samples were obtained from animals that had intraprostatic injection of LNCaP-luc-M6 cells. Using the DSL-10-9700 Active PSA kit (Diagnostic Systems Laboratory, Inc., Webster, TX), 25 µl of serum was analyzed by ELISA. The assay was performed according to the manufacturer's non-shaking assay protocol. Absorbance was read at 450 nm on a VERSAmax microplate reader (Molecular Devices, Sunnyvale, CA) and the data were collected and analyzed using SOFTmax Pro 3.1.2 software.

### Histopathology

Formalin fixed tissues were sent to IDEXX Veterinary Services, Inc. (West Sacramento, CA) for histopathological evaluation. Tissues were embedded, sectioned, and stained with hematoxylin and eosin (H&E).

### Statistical Analyses

The mean bioluminescence, mean tumor volume, and corresponding ± SEM were determined for the experiments. Regression plots were used to describe the relationship between bioluminescence, tumor volume, tumor weight, and serum PSA levels; $R^2$ values were used to assess the quality of the regression model.

### RESULTS

#### Stable Expression of Firefly Luciferase in the LNCaP-luc-M6 Cell Line

The firefly luciferase gene was transfected into LNCaP.FGC parental cells, and from the 48 bioluminescent colonies initially selected one colony that maintained stable constituitive luciferase expression was expanded to generate the stable LNCaP-luc-M6 cell
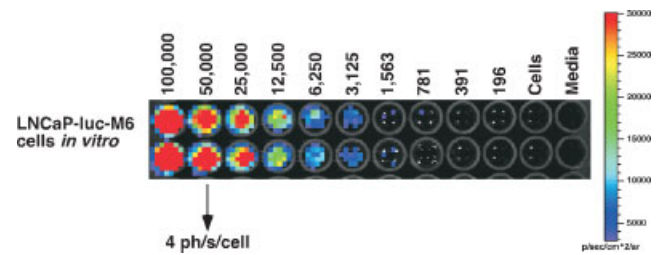


**Fig. I.** The in vitro bioluminescence of LNCaP-luc-M6 cells. Cells were serially diluted I:2 in a 96-well plate. Luciferin (I50 µg/ml) was added to the wells, and the plate was imaged for I min. Bioluminescence per well was quantified in photons/second (ph/sec), and the cells emit 4 ph/sec/cell.

line. The cell line was characterized in vitro to determine the level of bioluminescence. A suspension of LNCaP-luc-M6 cells was serially diluted into a 96-well plate and imaged (Fig. 1). The light emitted from the cells was approximately 4 ph/sec/cell, and the minimum number of detectable cells was between 1,500 and 3,000 cells per well.

#### LNCaP-luc-M6 Cells Retain the Androgen-Responsive Phenotype of Parental Cells

The LNCaP.FGC parental cell line expresses the androgen receptor and requires steroids for in vitro growth [6,7,9]. To confirm that the bioluminescent LNCaP-luc-M6 cell line retained this phenotype, protein extracts from the parental cells and LNCaP-luc-M6 cells were compared by Western analysis for androgen receptor expression (Fig. 2A). Since PC-3 cells express very low levels of androgen receptor mRNA and protein [31], the derivative cell line PC-3M-luc-C6 was also analyzed as a negative control. The results showed that LNCaP-luc-M6 cells express androgen receptor, and the level of expression was similar to the parental LNCaP.FGC cell line (Fig. 2A). Furthermore, when both LNCaP cell lines were grown in complete FBS-containing media, the parental and LNCaP-luc-M6 cells had similar doubling times (35 and 33 hr, respectively), and neither cell line proliferated in charcoal/dextran-treated serum-containing media with its reduced levels of steroids (Fig. 2B).

To determine whether the LNCaP-luc-M6 cells remained androgen-responsive following steroid deprivation, the androgen agonist R1881, shown to stimulate LNCaP cell proliferation in vitro [8,9,32,33], was added to the media. After 3 days, we found a 2.5-fold increase in the proliferation of LNCaP-luc-M6 cells exposed to R1881 (Fig. 2C). In addition, microscopic evaluation indicated that after R1881 addition, LNCaP-luc-M6 cells lost the elongated, neuronal-like morphology

**A**



**B**



**C**
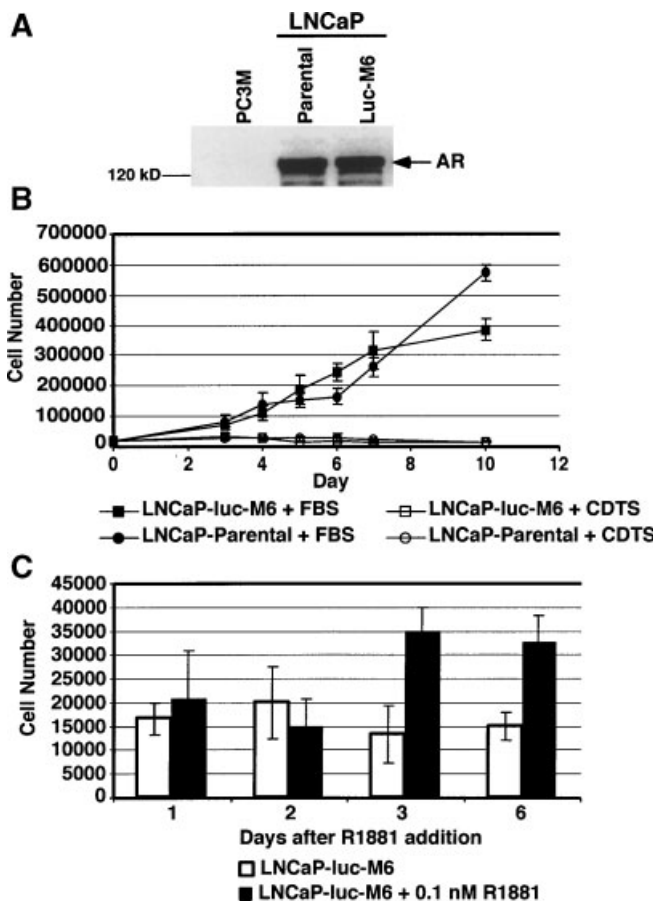


**Fig. 2.** LNCaP-luc-M6 cells express androgen receptor and need steroids for growth and proliferation in vitro. **A**: Protein lysate (25 μg) from PC3M-luc-C6 (PC3M), parental LNCaP.FGC (Parental), or LNCaP-luc-M6 (Luc-M6) cells was analyzed by Western blot for the androgen receptor (AR). **B**: On day 0, 20,000 cells/well were seeded in phenol red-free growth media with fetal bovine serum (FBS) or with charcoal/dextran-treated serum (CDTS). On the indicated days, wells (n = 3) were harvested and total cells counted. LNCaP-luc-M6 cells grown in FBS (■) or CDTS (□). Parental LNCaP.FGC was grown in FBS (●) or CDTS (○). Error bars represent standard error of the mean. Data shown are representative of two experiments. **C**: 20,000 cells/well were seeded in growth media with CDTS. Four days later the CDTS-containing media was replenished with or without the addition of the androgen agonist RI881 (0.1 nM). Wells (n = 3) were harvested and cells were counted on I, 2, 3, and 6 days after RI881 addition. Solid bars are LNCaP-luc-M6 cells grown in CDTS-media with RI881. Error bars represent standard error of the mean. Data shown are representative of two experiments.

LNCaP cells acquired when grown in media with charcoal-stripped serum (data not shown) [34].

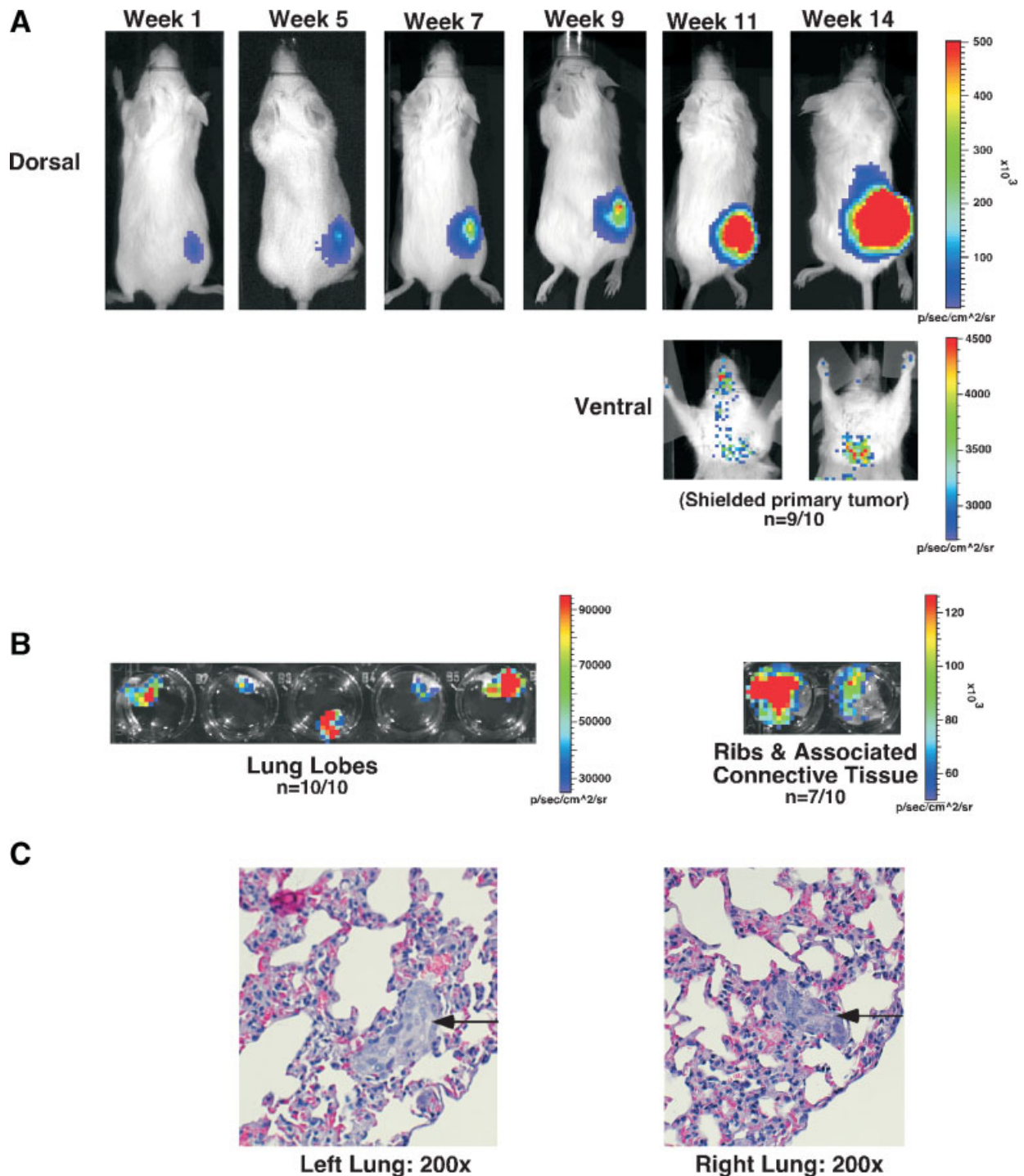## LNCaP-luc-M6 Cells as a Subcutaneous Model in SCID-bg Mice

The LNCaP-luc-M6 cells were injected at subcutaneous sites into male SCID-bg mice to assess tumor-

igenicity, and tumor growth was monitored by both BLI and caliper measurements (Figs. 3 and 4). As shown by a representative mouse in Figure 3A (dorsal view), tumor bioluminescence increased in animals over the course of several weeks. Inconsistencies in the growth of LNCaP subcutaneous tumors have been reported [6,7,10,14,15,18], and we did find that in three separate experiments, tumor take ratios varied from 35% to 100% (11/13, 10/10, and 6/17, data not shown). The mean photons emitted from the LNCaP-luc-M6 subcutaneous tumors of five animals over time are shown in Figure 4A. Tumor bioluminescence increased 4.3-fold in the first 6 weeks even though tumors were barely palpable, and the first measurement of tumor volume by calipers could not be obtained until after 7 weeks of tumor growth (Fig. 4B). From week 7–11, increases in tumor bioluminescence paralleled increases in tumor volume. After week 11, the tumor bioluminescence appeared to plateau, while tumor volume increased 3.3-fold. This plateau in bioluminescence in late stage tumors may reflect changes in tumor physiology that caliper measurements alone are unable to detect.

BLI has been successfully used to detect in vivo spontaneous metastases from primary xenograft tumors [27,30]. Although metastases from subcutaneous LNCaP tumors have not been reported, we used BLI to examine animals for the presence of spontaneous metastatic lesions. Ventral images of the animals were taken while the primary subcutaneous tumor was shielded in order to detect the relatively lower bioluminescence from metastatic lesions (Fig. 3A). As early as 7 weeks, indications of lung metastasis were seen in 2/10 animals in vivo by BLI, and by 11 weeks, pulmonary metastatic lesions were seen in 9/10 animals. When the animals were euthanized, the presence of metastases was confirmed by ex vivo imaging in lungs (10/10) and ribs with associated connective tissue (7/10) (Fig. 3B). When sections of lung lobes and ribs from selected animals were evaluated by histopathology, isolated micrometastases were identified in the lungs (Fig. 3C), while none could be identified in the ribs. Only 6–11 micrometastases were noted in the lung sections shown in Figure 3C explaining the relatively dim in vivo pulmonary signal in Figure 3A (bottom). It is possible that multiple rounds of histology would be required to eventually detect all the small micrometastases that were identified by ex vivo imaging.

## LNCaP-luc-M6 Cells as an Orthotopic Prostate Model in SCID-bg Mice

To study the orthotopic growth of LNCaP-luc-M6 prostate tumors in vivo by BLI, the cells were implanted in the dorsolateral prostate of male SCID-bg mice.

**Fig. 3.** In vivo imaging of LNCaP-luc-M6 subcutaneous tumors and pulmonary metastases in SCID-bg mice. Male mice received a subcutaneous injection of $3 \times 10^6$ LNCaP-luc-M6 cells suspended in 50% Matrigel. Animals were imaged weekly for 14 weeks. Data shown are representative of two experiments where tumor take rates were 11/13 and 10/10, respectively. **A**: Serial images of a representative mouse with a subcutaneous LNCaP-luc-M6 tumor. To check for metastasis development, animals were imaged on their ventral side, and the primary LNCaP-luc-M6 tumor was shielded. Metastases were detected by in vivo imaging in 9/10 animals. **B**: At the completion of the experiment, ex vivo imaging of excised tissues confirmed the presence of pulmonary metastatic lesions (10/10), as well as lesions in the ribs and associated connective tissue (7/10). **C**: A left and right lung with bioluminescent micrometastases was sectioned, stained (H&E), and photographed (200× magnification). Micrometastatic lesions were confirmed in these tissues and are indicated with an arrow.
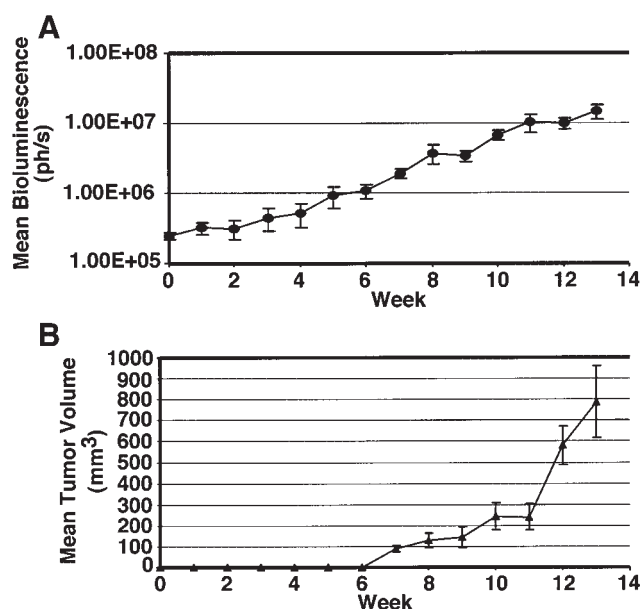
**Fig. 4.** Monitoring the bioluminescence and growth of subcutaneous LNCaP-luc-M6 tumors. Error bars represent standard error of the mean. **A**: Weekly measurements of mean bioluminescence from LNCaP-luc-M6 tumors (n = 5) in photons/second (ph/sec). **B**: Weekly mean caliper measurements of tumor volume (L × W × D) for the LNCaP-luc-M6 tumors (n = 5) in (A). Increases in mean tumor volume paralleled the increases detected in mean bioluminescence with a correlation of $R^2 = 0.78$.

Tumor growth in mice was monitored weekly in vivo by BLI and serum PSA levels. The images of a representative mouse in Figure 5A (top row) show that prostate tumor bioluminescence increased with time. Mean tumor bioluminescence increased exponentially after week 3, and at 16 weeks it was 43-fold higher than the level measured at the initial time point at week 1 (Fig. 6A). The levels of PSA in the serum of tumor-bearing animals were determined, and 6 weeks after implantation the mean PSA levels had risen approximately tenfold to 1 ng/ml (Fig. 6B). The serum PSA levels of tumor-bearing animals continued to increase over the next 10 weeks, and by 16 weeks the mean value had risen to 45 ng/ml, a level significantly higher than those found in tumor negative animals at 0.19 ng/ml. These increases in PSA corresponded to increases in bioluminescence ($R^2 = 0.87$). At week 16, the animals were euthanized, and the prostate tumors were removed and weighed. Animals with no bioluminescent signal were also euthanized for controls and confirmed negative for prostate tumor development.

Endpoint BLI data were compared to the traditional methods of monitoring intraprostatic tumor growth by serum PSA measurements and tumor weight. The data of two orthotopic LNCaP-luc-M6 experiments were pooled and compared (n = 12 mice). Endpoint biolu-

minescence correlated to both endpoint tumor weight (Fig. 7A, $R^2 = 0.82$) and to endpoint serum PSA levels (Fig. 7B, $R^2 = 0.83$). Similar correlations were found between endpoint tumor weight and endpoint serum PSA levels (Fig. 7C, $R^2 = 0.82$).

Since metastatic lesions have been reported with intraprostatic LNCaP tumors [7,12–14,16], animals with orthotopic LNCaP-luc-M6 prostate tumors were monitored for metastatic lesion development by BLI. Pulmonary metastases were detected in vivo in 5/12 animals with prostate tumors (Fig. 5A, bottom row). Metastases were detected as early as week 7 when the prostate tumor was shielded (data not shown). Once lung metastases were detected, the growth was monitored and quantified weekly with BLI (Fig. 6C). Bioluminescence above mean background signals ($5 \times 10^4$ ph/sec) was detected in all five mice when thoracic metastasis was first noted in the images. Subsequent quantification of thoracic bioluminescence generally showed a gradual or sharp increase in lung signal for at least two additional weeks or by the day of sacrifice. In all animals, when thoracic bioluminescence peaked the metastases had developed enough to be detected without shielding the primary tumor (Fig. 5A, top).

Ex vivo imaging of lung lobes and rib tissue confirmed the presence of bioluminescent metastases in the five animals identified by in vivo imaging and enhanced our ability to identify metastases in five additional tumor bearing animals (Fig. 5B). Sections of lungs and ribs from selected tumor-bearing animals were evaluated by histopathology, and numerous micrometastatic lesions were identified in the lungs (Fig. 5C), but as occurred with the subcutaneous tumor model, no micrometastases were found by histology in the rib sections. Prostate tumor burden did not predict whether an animal developed metastases as a mouse with a small 21 mg prostate tumor had confirmed lung and rib lesions by ex vivo imaging while another animal with a tumor five times larger showed no signs of metastasis by in vivo or ex vivo imaging (data not shown).

## DISCUSSION

In this study, we generated a bioluminescent line of LNCaP cells that are hormone-sensitive, retain the steroid-responsive phenotype of the parental cells and are useful for BLI studies of prostate cancer growth. LNCaP-luc-M6 cells expressed androgen receptor and secreted PSA. In addition, the LNCaP-luc-M6 cells required steroids for growth in vitro, similar to reports describing the parental LNCaP cell line [7–9]. In our studies, steroid-deprived LNCaP-luc-M6 cells responded to androgen agonist-supplemented media
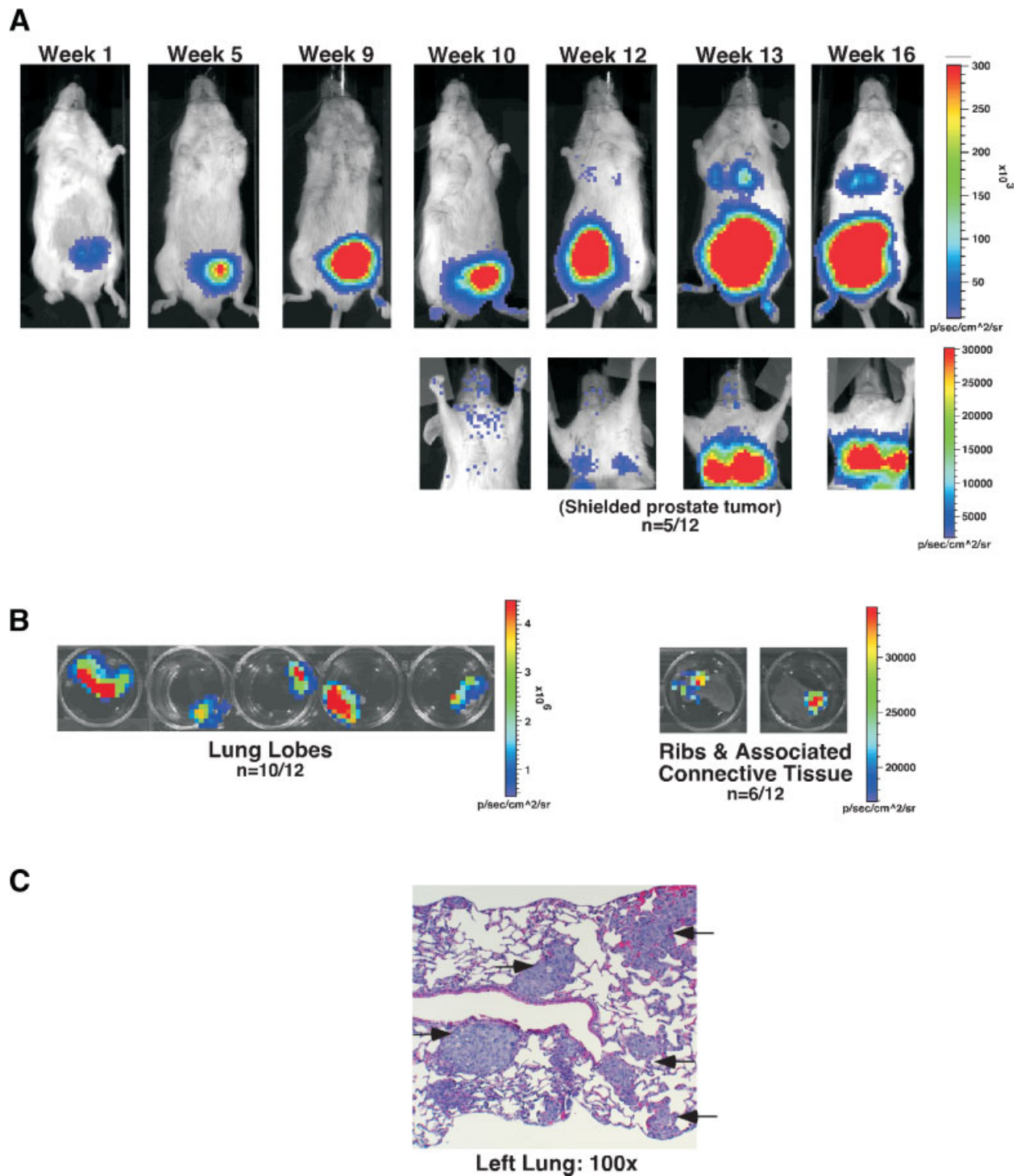
**Fig. 5.** In vivo imaging of orthotopic LNCaP-luc-M6 prostate tumors and pulmonary metastases in SCID-bg mice. Male mice received an intraprostatic injection of $1 \times 10^6$ LNCaP-luc-M6 cells and were imaged once a week for 16 weeks. Data shown are representative of two experiments where the rates of prostate tumor take were 4/8 and 8/10, respectively. **A**: Selected images of a representative mouse with a LNCaP-luc-M6 prostate tumor. To check for metastasis development, animals were imaged with the primary prostate tumor shielded. In vivo imaging detected possible pulmonary metastases in 5/12 animals. **B**: At the completion of the experiment, ex vivo imaging confirmed the growth of pulmonary metastatic lesions (10/12), as well as lesions in the ribs and associated connective tissue (6/12). **C**: A left lung with bioluminescent micrometastases was sectioned, stained (H&E), and photographed (100× magnification). Micrometastatic lesions were confirmed in this tissue and are indicated with arrows.
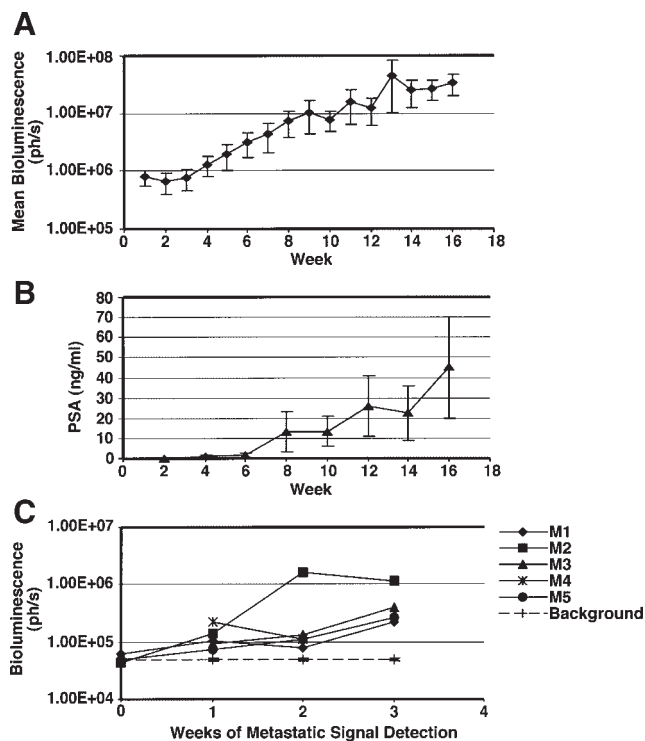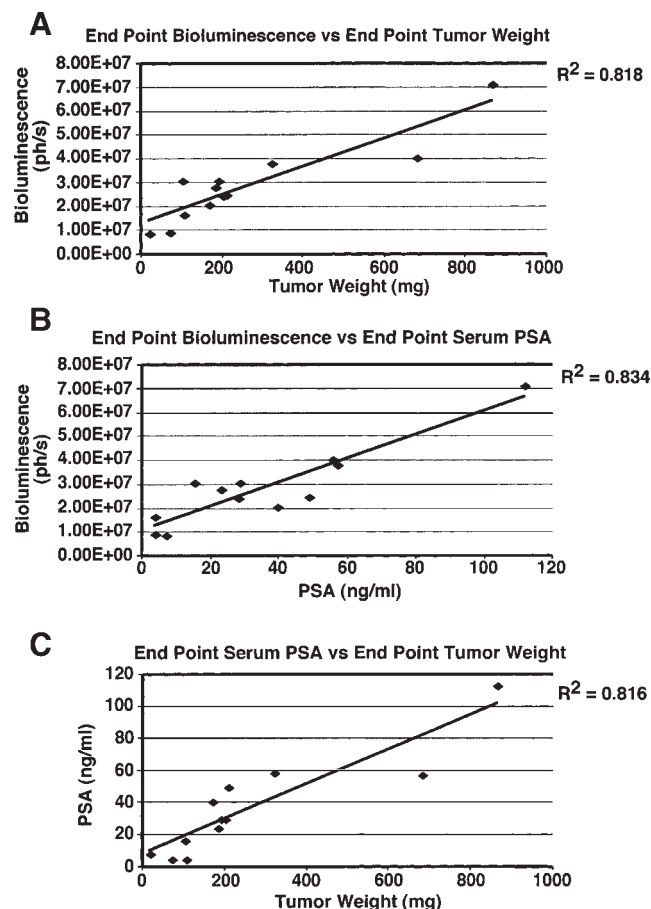
**Fig. 6.** Monitoring the bioluminescence and growth of orthotopic LNCaP-luc-M6 tumors and metastatic lesions. Data shown are representative of two experiments. Error bars represent standard error of the mean. **A**: Weekly measurements of mean bioluminescence from LNCaP-luc-M6 prostate tumors (n = 4) in photons/second (ph/sec). **B**: Circulating mean PSA levels (ng/ml) are shown for the animals in A (n = 4). Increases in mean tumor bioluminescence correlated with increases in mean serum PSA levels ($R^2 = 0.86$). **C**: Measurement of bioluminescent pulmonary metastases in photons/second (ph/sec) from animals (n = 5) with visually evident in vivo metastasis. Week 1 is the first imaging timepoint where metastases were detected for each mouse. Data is from two experiments. Background: mean bioluminescence from the thoracic cavity of metastasis-negative mice. M, mouse.



**Fig. 7.** Comparing bioluminescent imaging to the current methods of monitoring intraprostatic tumor growth. Endpoint data from two experiments were analyzed (n = 12 mice). **A**: The endpoint bioluminescence was compared to endpoint tumor weights. **B**: The endpoint bioluminescence was compared to endpoint serum PSA levels. **C**: The endpoint serum PSA levels were compared to endpoint tumor weights. The correlations were similar for all three comparisons.

with an increase in cellular proliferation within 3 days. A similar increase in proliferation has been reported for parental LNCaP cells treated with R1881 [8,32,33]. It is noteworthy that the androgen receptor in LNCaP cells has a mutation in the ligand binding domain, allowing the receptor to be activated by other steroids and some anti-androgens [35,36]. Since similar mutations have been identified in prostate cancer patients [37,38], the LNCaP-luc-M6 cell line offers promise in testing new therapies aimed at tumors reflecting this important clinical subgroup.

We found that the take rate of LNCaP-luc-M6 subcutaneous tumors in male SCID-bg mice varied from 35% to 100% between experiments. Such inconsistent subcutaneous growth has been well documented in the parental LNCaP cells, with one study citing

successful tumor take in as few as 1/10 animals [7]. The inclusion of Matrigel or human bone fibroblasts has been shown to considerably improve the subcutaneous tumor growth of LNCaP cells [10,11,14,17], and we did use Matrigel in our experiments. The more limited success (6/17) in one of our experiments may have been related to insufficient testosterone levels within the male mice used for that experiment. It has been shown that LNCaP tumor take rates dramatically decrease in animals with reduced testosterone levels [6,7].

In both the LNCaP-luc-M6 subcutaneous and orthotopic models, increases in tumor growth were detected earlier when measured by BLI than by the traditional methods of caliper measurement or serum PSA analysis. In some instances, subcutaneous LNCaP-luc-M6 tumors were measurable by caliper only for a

short time before the animal succumbed to complications related to pulmonary metastases. In these same animals, we successfully assessed primary tumor growth by BLI for 6 weeks before any symptoms appeared. Once measurable by calipers, mean increases in tumor volume paralleled the increases in mean tumor bioluminescence. Serum PSA levels also mirrored photon measurements over time, and we found that endpoint LNCaP-luc-M6 prostate tumor bioluminescence correlated with endpoint serum PSA levels.

Previous studies have shown metastasis to lymph nodes and lungs of mice with orthotopic LNCaP prostate tumors [7,12–14,16]. There have been no reports of metastases from subcutaneous LNCaP tumors. In our studies, metastases were detected in the lungs, ribs, preputial gland, connective tissue, and lymph nodes of SCID-bg mice with subcutaneous and orthotopic LNCaP-luc-M6 tumors. Furthermore, we were able to detect pulmonary metastases at very early time points in vivo and monitor the growth of these lesions continually for several weeks. In some of the animals with orthotopic LNCaP-luc-M6 tumors, ex vivo analysis of lung lobes enhanced metastatic detection and increased the total number of animals with bioluminescent lung signals from 5/12 to 10/12. Pulmonary lesions have been reported in animals with androgen-dependent LAPC-4 xenograft tumors when BLI was combined with administration of a luciferase-expressing adenovirus [30]. In these studies as in ours, ex vivo imaging confirmed the localization of the metastases and dictated which tissues would be analyzed by histopathology.

The current treatment protocol for patients with androgen-dependent prostate cancer is chemical or surgical castration. Following tumor regression, more often than not the tumors regrow even in the absence of androgens, although some of these androgen-independent prostate tumors may still be sensitive to hormone manipulations [2]. The need exists for animal models that recapitulate the progression of hormone-sensitive early prostate cancer to its more aggressive, androgen-independent state. With the bioluminescent LNCaP-luc-M6 cell line, prostate tumor regression and regrowth can be imaged in vivo and used to assess new hormone-related therapies for treating primary as well as metatstatic disease. Derivative LNCaP cell lines have been generated that represent different stages in prostate cancer progression. These derivative cell lines are often generated by culturing LNCaP cells isolated from primary or metastatic tumors grown in intact or castrated male mice [4,5,7,39]. Since we show that the bioluminescence of LNCaP-luc-M6 cells is maintained in vivo, a similar strategy of isolating LNCaP-luc-M6 cells from an orthotopic or metastatic lesion could be employed with the potential to generate derivative cell lines with different androgen sensitivities and metastatic capabilities.

A recent animal study described the spontaneous development and detection of pituitary tumors using BLI and transgenic mouse technology [22]. The various stages in prostate cancer progression are now being investigated using transgenic mouse models, but studies are limited to traditional endpoint methods of tumor growth analysis [40]. Creating a transgenic mouse model of spontaneous prostate cancer with bioluminescent tumors would facilitate in vivo monitoring of disease progression and metastasis detection. Patterns of gene expression could also be compared between the primary tumor and metastases and to help identify genes contributing to the development of metastatic prostate cancer.

## CONCLUSIONS

With improvements in imaging modalities, previously elusive properties of tumor biology are now more detectable and measurable. Monitoring primary tumor growth, the status of residual disease, and the development of metastatic disease are currently possible in vivo with the use of small animal imaging technologies including BLI. The development of bioluminescent tumor models, including the human LNCaP-luc-M6 cell line reported in this study, improves upon traditional methodologies to provide early and sensitive assessment of treatment regimens.

## ACKNOWLEDGMENTS

## REFERENCES

1. Jemal A, Murray T, Samuels A, Ghafoor A, Ward E, Thun MJ. Cancer statistics, 2003. CA Cancer J Clin 2003;53:5–26.

2. Oh WK, Hurwitz M, D'Amico AV, Richie JP, Kantoff PW. Neoplasms of the prostate. In: Emil Frei I, editor. Cancer medicine e.5. Hamilton, Ontario, Canada: B.C. Decker, Inc.; 2000. pp 1559–1588.

3. Lee C, Shevrin DH, Kozlowski JM. In vivo and in vitro approaches to study metastasis in human prostatic cancer. Cancer Metastasis Rev 1993;12:21–28.

4. van Weerden WM, Romijn JC. Use of nude mouse xenograft models in prostate cancer research. Prostate 2000;43:263–271.

5. Navone NM, Logothetis CJ, Eschenbach ACv, Troncoso P. Model systems of prostate cancer: Uses and limitations. Cancer Metastasis Rev 1999;17:361–371.

6. Horoszewicz JS, Leong SS, Kawinski E, Karr JP, Rosenthal H, Chu TM, Mirand EA, Murphy GP. LNCaP model of human prostatic carcinoma. Cancer Res 1983;43:1809–1818.

7. Pettaway CA, Pathak S, Greene G, Ramirez E, Wilson MR, Killion JJ, Fidler IJ. Selection of highly metastatic variants of different human prostatic carcinomas using orthotopic implantation in nude mice. Clin Cancer Res 1996;2:1627–1636.

8. van Steenbrugge GJ, van Uffelen CJ, Bolt J, Schroder FH. The human prostatic cancer cell line LNCaP and its derived sublines: An in vitro model for the study of androgen sensitivity. J Steroid Biochem Mol Biol 1991;40:207–214.

9. Langeler EG, van Uffelen CJ, Blankenstein MA, van Steenbrugge GJ, Mulder E. Effect of culture conditions on androgen sensitivity of the human prostatic cancer cell line LNCaP. Prostate 1993;23:213–223.

10. Lim DJ, Liu XL, Sutkowski DM, Braun EJ, Lee C, Kozlowski JM. Growth of an androgen-sensitive human prostate cancer cell line, LNCaP, in nude mice. Prostate 1993;22:109–118.

11. Gleave M, Hsieh JT, Gao CA, von Eschenbach AC, Chung LW. Acceleration of human prostate cancer growth in vivo by factors produced by prostate and bone fibroblasts. Cancer Res 1991;51:3753–3761.

12. Maeda H, Segawa T, Kamoto T, Yoshida H, Kakizuka A, Ogawa O, Kakehi Y. Rapid detection of candidate metastatic foci in the orthotopic inoculation model of androgen-sensitive prostate cancer cells introduced with green fluorescent protein. Prostate 2000;45:335–340.

13. Rembrink K, Romijn JC, van der Kwast TH, Rubben H, Schroder FH. Orthotopic implantation of human prostate cancer cell lines: A clinically relevant animal model for metastatic prostate cancer. Prostate 1997;31:168–174.

14. Sato N, Gleave ME, Bruchovsky N, Rennie PS, Beraldi E, Sullivan LD. A metastatic and androgen-sensitive human prostate cancer model using intraprostatic inoculation of LNCaP cells in SCID mice. Cancer Res 1997;57:1584–1589.

15. Stephenson RA, Dinney CP, Gohji K, Ordonez NG, Killion JJ, Fidler IJ. Metastatic model for human prostate cancer using orthotopic implantation in nude mice. J Natl Cancer Inst 1992;84:951–957.

16. Wang X, An Z, Geller J, Hoffman RM. High-malignancy orthotopic nude mouse model of human prostate cancer LNCaP. Prostate 1999;39:182–186.

17. Gleave ME, Hsieh JT, von Eschenbach AC, Chung LW. Prostate and bone fibroblasts induce human prostate cancer growth in vivo: Implications for bidirectional tumor-stromal cell interaction in prostate carcinoma growth and metastasis. J Urol 1992;147:1151–1159.

18. Gleave ME, Hsieh JT, Wu HC, von Eschenbach AC, Chung LW. Serum prostate specific antigen levels in mice bearing human prostate LNCaP tumors are determined by tumor volume and endocrine and growth factors. Cancer Res 1992;52:1598–1605.

19. Weissleder R. Scaling down imaging: Molecular mapping of cancer in mice. Nat Rev Cancer 2002;2:11–18.

20. Sweeney TJ, Mailander V, Tucker AA, Olomu AB, Zhang W, Cao Y, Negrin RS, Contag CH. Visualizing the kinetics of tumor-cell clearance in living animals. Proc Natl Acad Sci USA 1999;96:12044–12049.

21. Edinger M, Sweeney TJ, Tucker AA, Olomu AB, Negrin RS, Contag CH. Noninvasive assessment of tumor cell proliferation in animal models. Neoplasia 1999;1:303–310.

22. Vooijs M, Jonkers J, Lyons S, Berns A. Noninvasive imaging of spontaneous retinoblastoma pathway-dependent tumors in mice. Cancer Res 2002;62:1862–1867.

23. Rehemtulla A, Stegman LD, Cardozo SJ, Gupta S, Hall DE, Contag CH, Ross BD. Rapid and quantitative assessment of cancer treatment response using in vivo bioluminescence imaging. Neoplasia 2000;2:491–495.

24. Bhaumik S, Gambhir SS. Optical imaging of *Renilla* luciferase reporter gene expression in living mice. Proc Natl Acad Sci USA 2002;99:377–382.

25. Contag CH, Jenkins D, Contag PR, Negrin RS. Use of reporter genes for optical measurements of neoplastic disease in vivo. Neoplasia 2000;2:41–52.

26. Edinger M, Cao YA, Hornig YS, Jenkins DE, Verneris MR, Bachmann MH, Negrin RS, Contag CH. Advancing animal models of neoplasia through in vivo bioluminescence imaging. Eur J Cancer 2002;38:2128–2136.

27. El Hilali N, Rubio N, Martinez-Villacampa M, Blanco J. Combined noninvasive imaging and luminometric quantification of luciferase-labeled human prostate tumors and metastases. Lab Invest 2002;82:1563–1571.

28. Wetterwald A, van der Pluijm G, Que I, Sijmons B, Buijs J, Karperien M, Lowik CW, Gautschi E, Thalmann GN, Cecchini MG. Optical imaging of cancer metastasis to bone marrow: A mouse model of minimal residual disease. Am J Pathol 2002;160:1143–1153.

29. Iyer M, Wu L, Carey M, Wang Y, Smallwood A, Gambhir SS. Two-step transcriptional amplification as a method for imaging reporter gene expression using weak promoters. Proc Natl Acad Sci USA 2001;98:14595–14600.

30. Adams JY, Johnson M, Sato M, Berger F, Gambhir SS, Carey M, Iruela-Arispe ML, Wu L. Visualization of advanced human prostate cancer lesions in living mice by a targeted gene transfer vector and optical imaging. Nat Med 2002;8:891–897.

31. Lin MF, Meng TC, Rao PS, Chang C, Schonthal AH, Lin FF. Expression of human prostatic acid phosphatase correlates with androgen-stimulated cell proliferation in prostate cancer cell lines. J Biol Chem 1998;273:5939–5947.

32. Berns EM, de Boer W, Mulder E. Androgen-dependent growth regulation of and release of specific protein(s) by the androgen receptor containing human prostate tumor cell line LNCaP. Prostate 1986;9:247–259.

33. Cleutjens CB, Steketee K, van Eekelen CC, van der Korput JA, Brinkmann AO, Trapman J. Both androgen receptor and glucocorticoid receptor are able to induce prostate-specific antigen expression, but differ in their growth-stimulating properties of LNCaP cells. Endocrinology 1997;138:5293–5300.

34. Saeed B, Zhang H, Ng SC. Apoptotic program is initiated but not completed in LNCaP cells in response to growth in charcoal-stripped media. Prostate 1997;31:145–152.

35. Veldscholte J, Ris-Stalpers C, Kuiper GG, Jenster G, Berrevoets C, Claassen E, van Rooij HC, Trapman J, Brinkmann AO, Mulder E. A mutation in the ligand binding domain of the androgen receptor of human LNCaP cells affects steroid binding characteristics and response to anti-androgens. Biochem Biophys Res Commun 1990;173:534–540.

36. McDonald S, Brive L, Agus DB, Scher HI, Ely KR. Ligand responsiveness in human prostate cancer: Structural analysis of

mutant androgen receptors from LNCaP and CWR22 tumors. Cancer Res 2000;60:2317–2322.

37. Shi XB, Ma AH, Xia L, Kung HJ, de Vere White RW. Functional analysis of 44 mutant androgen receptors from human prostate cancer. Cancer Res 2002;62:1496–1502.

38. Taplin ME, Bubley GJ, Shuster TD, Frantz ME, Spooner AE, Ogata GK, Keer HN, Balk SP. Mutation of the androgen-receptor gene in metastatic androgen-independent prostate cancer. N Engl J Med 1995;332:1393–1398.

39. Chung LW, Zhau HE, Wu TT. Development of human prostate cancer models for chemoprevention and experimental therapeutics studies. J Cell Biochem Suppl 1997;28–29:174–181.

40. Abate-Shen C, Shen MM. Mouse models of prostate carcinogenesis. Trends Genet 2002;18:S1–S5.